REFLECTANCE OF MERCURY'S POLAR REGIONS: CALIBRATION AND IMPLICATIONS FOR MERCURY'S VOLATILES. G. A. Neumann[1], X. Sun[1], A. Cao[2], A. N. Deutsch[3], and J. W. Head[3], [1]NASA Goddard Space Flight Center, Greenbelt, MD 20771, USA (email: gregory.a.neumann@nasa.gov), [2]University of Washington, Seattle WA 98195, USA, [3]Department of Earth, Environmental and Planetary Sciences, Brown University, Providence, RI 02912, USA. [4]Department of Earth, Atmospheric and Planetary Sciences, Massachusetts Institute of Technology, Cambridge, Massachusetts 02139-4307, USA.

Introduction: The Mercury Laser Altimeter (MLA) [1] on board the MESSENGER spacecraft measured the outgoing and returned energy of 1064-nm-wavelength laser pulses reflected from the surface, as well as precise time-of-flight ranges. These ancillary measurements were interpreted via a link equation [2] as reflectances relative to Lambertian. The measurement precision of ~25% was best in a nadir geometry, where the height of pulses could be sensed at two separate threshold voltages, however most observations in the polar regions were necessarily oblique to the surface normal. Understanding the interaction of the laser beam at zero phase angle (the angle between incident and emitted light) is critical for understanding the composition and properties of the regolith on airless bodies, e.g., [3], and for characterizing volatile processes in permanently shadowed regions [4-9]. The energy in obliquely incident returns is dispersed over a greater interval of time than the incident pulse [10], with reduced amplitude. This poses a challenge to accurate calibration of data acquired over the course of 4+ years of operation at distances varying by orders of magnitude. As well, the systematic changes in the laser beam itself must be considered in the link equation.

Implications for Mercury's Volatiles: The importance of this work to understanding the distribution and emplacement history of volatiles warrants further attention to the calibration of reflectance under varying conditions. In the cold traps on Mercury, the distribution of both bright and dark materials has been obtained from scattered light images within persistently shadowed regions [11] but the images are highly stretched and not calibrated to reflectance. Distinct margins between regolith and lag deposits are resolved by images, and a few images also see the margins between regolith and bright deposits, but the stratigraphy of both types of volatiles is not resolved within the same image. Poleward darkening of the regolith can be interpreted as increasing population of sublimation lag deposits [12], while brightening poleward, even excluding well-resolved craters, has been attributed to patches of ice exposed at the kilometer scale resolution of the MLA data [13]. However the MLA dataset archived in the PDS [14] has systematic biases northward of the 84° orbital inclination of MESSENGER.

An engineering model of the MLA instrument (delivered in 2003) still operates as a test bed for calibrations (Fig. 1). Signals from a laser diode can be controlled digitally with arbitrary waveforms fed into a flight-like avalanche photodiode detector. The timing circuitry is also identical that used to measure the pulse energy on MLA [8]. We have examined the range precision and differential pulse widths obtained over 40 dB of signal attenuation from saturation to extinction and can now assess the factors that account for systematic biases (Fig. 2). Further work using this system and calibration progress will be presented.

References:

[1] Cavanaugh J. F. et al. (2007) *Space Sci. Rev., 131*, 451-479. [2] Sun X. and Neumann G. A. (2015) *IEEE Trans. Geosci. Rem. Sens.*, *53*, 2860–2874. [3] Barker M. K. et al. (2015) *Icarus, 273*, 96–113. [4] Zuber M. T. et al. (2012) *Nature, 486*, 378–381. [5] Lucey P. G. et al. (2014) *JGR Planets*, *119,* 1665–1679 [6] Lemelin, M. et al. (2016) *Icarus 273*, 315–328. [7] Fisher E. et al. (2017) *Icarus, 292*, 74–85. [8] Neumann G. A. et al. (2013) *Science, 339, 296–300.* [9] Deutsch A. N. et al. (2017) *Icarus, 280,* 158–171. [10] Gardner C. S. (1992) *IEEE Trans. Geosci. Rem. Sens. 30*, 1061-1072. [11] Chabot N. L. et al. (2014) *Geology, 42,* 1051-1054. [12] Rubanenko L. et al. (2018) *this meeting*. [13] Chabot N. L. et al. (2018) *this meeting*. [13] Deutsch A. N. et al. (2017) *GRL 44*, 9233-9241. [14] Dataset mess-e_v_h-mla-3_4-cdr_rdr-data-v1 at pds-geosciences.wustl.edu/messenger/.

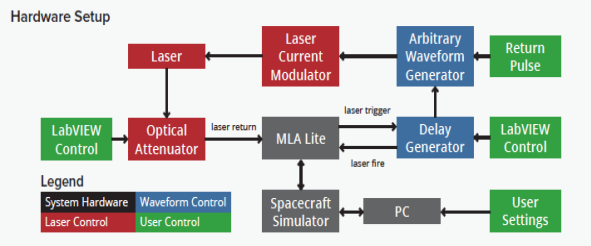

Figure 1: Instrument test setup block diagram.

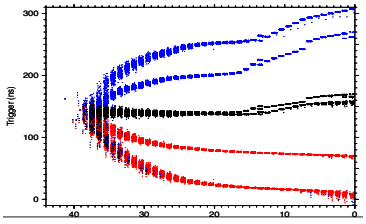

Figure 2: Leading and trailing edge pulse timings vs. attenuation at dual thresholds, used to infer energy.